

# Photoionization of HBr and DBr near threshold

B. Ruscic and J. Berkowitz

Chemistry Division, Argonne National Laboratory, Argonne, Illinois 60439

(Received 13 March 1990; accepted 18 April 1990)

Photoionization is observed in HBr (at 300 K) below the adiabatic threshold. The photoion yield curve has structure, and is independent of both pressure and electric field over a large range. The peaks can be simulated rather well by a model which assumes rotational autoionization, with  $\Delta N \approx -4$ . This model does not exclude concomitant processes with  $\Delta N = -1, -2, -3$ . A formal theory is also presented, which describes  $\Delta N = -4$  as occurring through successive quadrupole transitions, in second-order perturbation theory. A tentative conclusion is drawn, based on preliminary studies of other molecules, that a type of rotational autoionization can occur in heteronuclear diatomic molecules without an electric field, and in homonuclear diatomic molecules with such a field. The photoionization of DBr has been studied with similar conditions. A corresponding simulation is in good agreement with the observed structure below the adiabatic threshold. In addition, one peak in a triad observed in HBr above threshold, and predicted by an MQDT calculation to be absent in DBr, is still observed.

## I. INTRODUCTION

It is often observed in molecular photoionization studies that significant ionization occurs below threshold, where threshold is determined by some other technique, and is assumed to be the transition from the lowest rovibronic state of the neutral molecule to the lowest corresponding state of the molecular ion. Various reasons are offered, including collisional effects on high Rydberg states, electric field effects and hot bands. One recent example<sup>1</sup> is that of HBr, which was measured at a sample temperature of  $-120^\circ$ . The ionization threshold deduced from electron impact excitation spectroscopy<sup>2</sup> is  $11.66 \pm 0.01$  eV  $\equiv 1063.3 \pm 0.9$  Å, and the value given by Huber and Herzberg<sup>3</sup> is 11.67 eV, whereas in the above cited photoionization mass spectrometric study some ionization is observed at  $1066$  Å  $\equiv 11.63$  eV. The authors<sup>1</sup> state that "...the ionization observed... at wavelengths longer than  $1063.3$  Å is due primarily to collisional ionization of Rydberg states converging to the  $^2\Pi_{3/2}, v^+ = 0$  ionization limit."

We had recently studied<sup>4</sup> the photoionization spectrum of the homonuclear species  $N_2$  at and below threshold. We observed structure which was attributed to rotational autoionization in the presence of an electric field of  $\sim 13$  V/cm, which was not prominent at a field of  $\sim 1$  V/cm. In these studies, the observed structure was not pressure dependent, and hence could not be attributed to collisional ionization of Rydberg states. We considered the possibility that the electric field was necessary in the  $N_2$  studies because of the absence of a permanent electric dipole moment in that species and speculated that a heteronuclear diatomic molecule might exhibit such rotational autoionization without the mediation of an electric field. HBr was a convenient molecule for these studies, because it has a permanent electric dipole moment (0.82 D),<sup>5</sup> and a fairly large rotational constant.<sup>3</sup> In the course of these studies, we could test the influence of collisional ionization, as well as electric field effects, in the subthreshold region.

Some additional studies were performed with DBr. If

rotational autoionization were occurring, the smaller rotational constant of DBr should manifest itself as a change in the subthreshold spectrum. Another reason for examining DBr relates to the multichannel quantum defect (MQDT) analysis of the HBr spectrum presented by Lefebvre-Brion *et al.*<sup>1</sup> In the near (but above) threshold region of the HBr spectrum, there are *three* autoionization peaks between  $\sim 1058$ – $1060$  Å. From their MQDT analysis of the HBr spectrum, Lefebvre-Brion *et al.* concluded that in DBr "... it is expected that the third peak calculated at  $1059.7$  Å, will disappear." Their calculated spectrum for DBr in this region (their Fig. 3) displays *two* peaks. A scan of this region with both HBr and DBr at similar conditions could test their prediction.

## II. EXPERIMENTAL ARRANGEMENT

The experimental apparatus, consisting basically of a 3 m normal incidence vacuum ultraviolet monochromator and a quadrupole mass spectrometer, has been described previously.<sup>6</sup> The sample gases (HBr and DBr) were intentionally studied at room temperature, rather than at a cooler temperature, to enhance the population of higher rotational levels. The principal light source utilized in these studies was the argon continuum, in order to minimize the occurrence of false structure. The resolution employed was  $0.14$  Å (FWHM). The argon continuum is heavily self-absorbed at the resonance line of Ar,  $1066.660$  Å. Hence, there is a gap in our data, encompassing  $\sim 1$  Å near this line. However, by changing to low pressure lamp conditions, one can utilize this line as an accurate calibration of the wavelength scale. The accuracy can be expected to diminish slightly as the measured spectra depart from this fixed point. DBr was obtained from ICON.

## III. EXPERIMENTAL RESULTS

### A. Pressure effects

The photoionization spectrum of HBr at 300 K in the near threshold region is shown for three pressures of sample

gas in Fig. 1. It extends to at least 1070 Å. The structural features observed in this spectrum are reproducible. Furthermore, they do not change significantly ( $\leq 10\%$ ) over a pressure range of more than a factor of 50. Therefore, we conclude that collisional ionization of Rydberg states is an unlikely explanation for this structure below threshold.

### B. Electric field effects

The same region of the HBr spectrum was scanned with electric fields in the ionization region varying from 0.83 to 53.3 V/cm. There was no significant change in the positions or relative intensities of the structural features, unlike the previously studied spectrum of  $N_2$ .<sup>4</sup>

### C. Isotopic effects

The photoionization spectrum of DBr is shown in Fig. 2, juxtaposed with a spectrum of HBr obtained under the same conditions. These spectra extend to the region above threshold, where MQDT analysis predicted the absence of one peak in a triad.<sup>1</sup> It can be seen that all three peaks are present in both HBr and DBr. In fact, the highest peak in the triad in DBr is the one expected to be absent. (The offset is attributed to the slightly higher ionization potential of DBr compared to HBr.) The region below threshold displays structure similar to that found in HBr.

## IV. INTERPRETATION OF RESULTS

The absence of significant pressure effects argues against the earlier conclusion<sup>1</sup> that ionization at wavelengths longer than 1063.3 Å is due primarily to collisional ionization of Rydberg states. The structural features are

more likely unimolecular, rather than bimolecular (pseudo-unimolecular) in nature. The absence of significant electric field effects, down to 0.83 V/cm, implies that these unimolecular features are at most very slightly influenced by the presence of a field. In a similar study of  $N_2$ ,<sup>4</sup> structural features began to appear at fields about ten times stronger than the lowest field employed here. Since the energy required for ionization below threshold is not being supplied by collisions, nor by an electric field, it must be contained within the molecules. The Boltzmann ratio of  $v'' = 1$  to  $v'' = 0$  is less than  $10^{-5}$  for HBr at 300 K. Clearly, the most likely source of this energy is contained in the Boltzmann population of rotational states. One or more quanta of rotational energy of the  $HBr^+$  core must be transferred to the Rydberg electron, enabling it to escape. In our previous study on  $N_2$ , the absence of a permanent dipole moment implied that the lowest order of interaction between the Rydberg electron and its core was quadrupolar, and consequently a minimum of two units of rotational angular momentum (and only even units) could be transferred. In the present case, we must consider all possibilities.

### A. Simulation of the experimental results

Before embarking upon a theoretical development, we adopt a more pragmatic approach. First, we compute the rotational energies of HBr,  $X^1\Sigma^+$ , and  $HBr^+$ ,  $X^2\Pi_{3/2}$ , using rather well-established rotational constants.<sup>3</sup> Then assuming 11.66 eV to be the ionization energy from the lowest rotational state of HBr to the lowest rotational state of  $HBr^+$ , we calculate the ionization energies for the higher rotational states, with  $P$ ,  $Q$  and  $R$  branches. Next, we consider Rydberg series converging to these various limits. Their energies are calculated from the Rydberg formula, utilizing

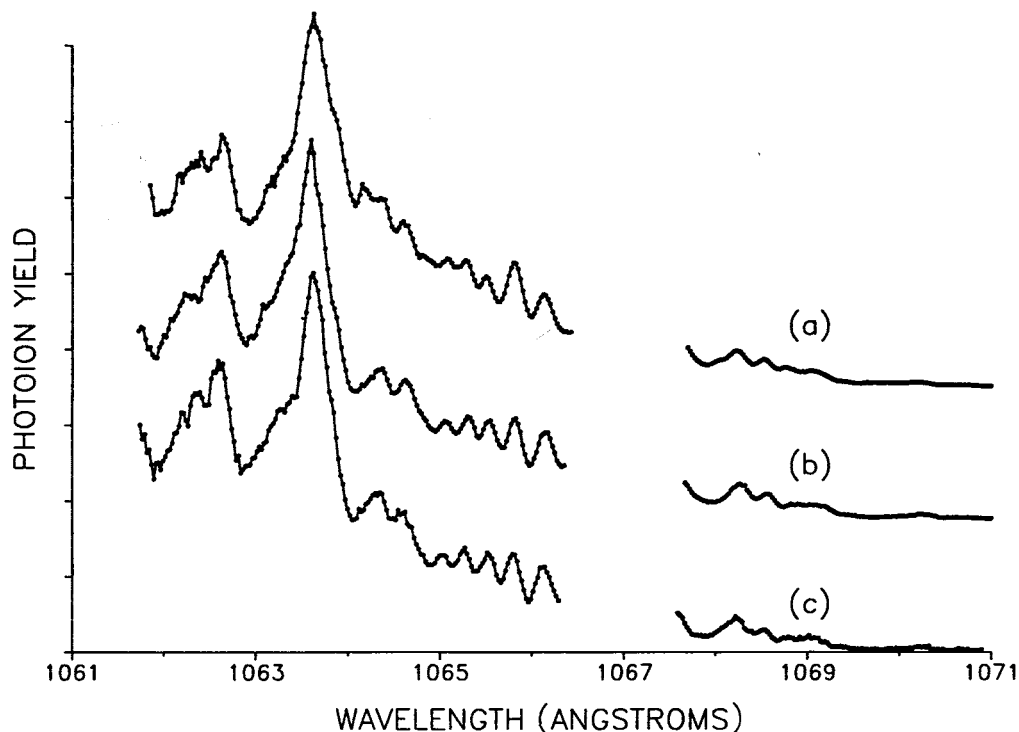


FIG. 1. Photoionization spectrum of HBr, at 300 K, in the near-threshold region. (a)  $P \approx 1$  mTorr; (b)  $P \approx 0.1$  mTorr; (c)  $P \approx 0.02$  mTorr. The gap in the spectra corresponds to the gap in the argon continuum light source.

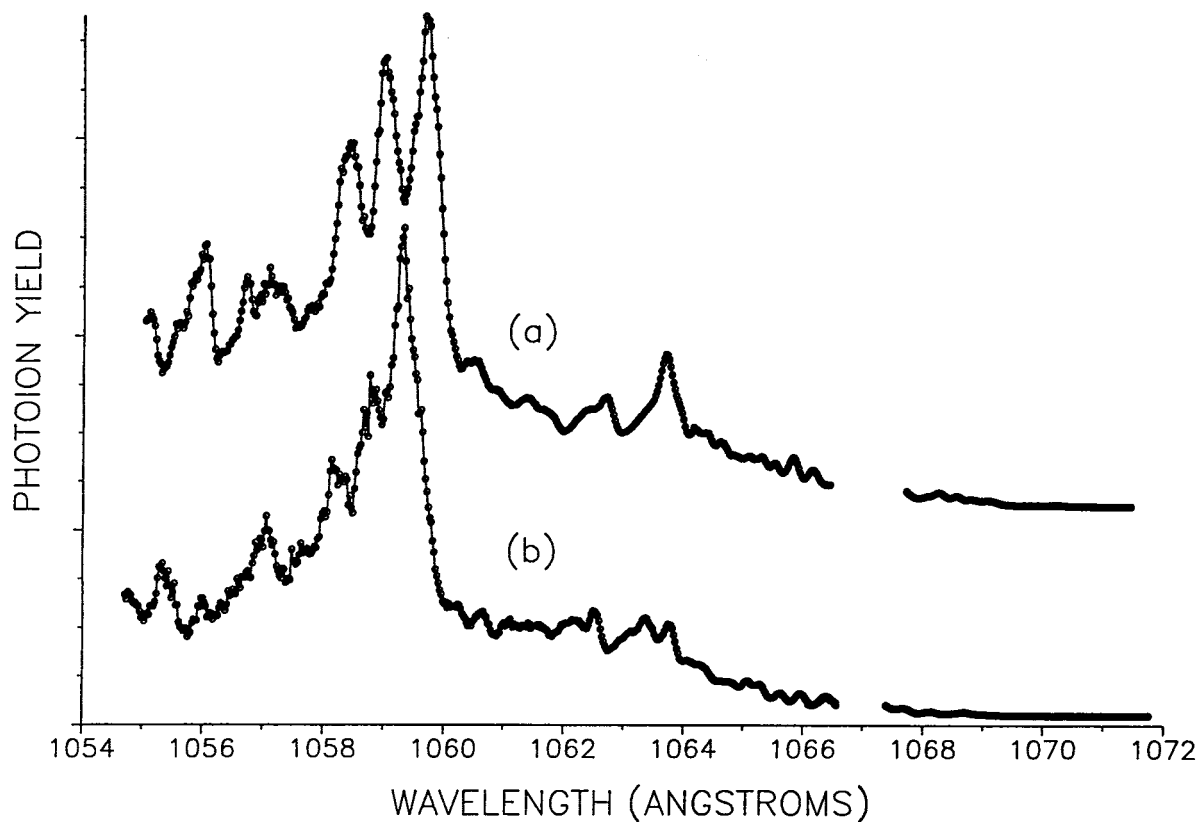


FIG. 2. Photoion yield curves of HBr and DBr in the region below and above threshold, demonstrating the presence of a triad of peaks above threshold in both HBr and DBr. (a) HBr; (b) DBr.

the quantum defect  $\delta = 3.08$  obtained by Shaw *et al.*<sup>2</sup> from their electron impact excitation study. A similar value of  $\delta$  for ns transitions has been observed in this laboratory for atomic bromine.<sup>7</sup> (At this point, the value of  $\delta$  used is an estimate, since the highest Rydberg member identified by Shaw *et al.* corresponds to  $n = 9$ , and we shall be invoking higher principal quantum numbers). Some of these Rydberg terms converging to  $N'$  will lie above the limit for  $N' - 1$ . Energetically, they can transfer one unit of rotational angular momentum to the Rydberg electron, enabling ionization to occur. A larger number of members of the same Rydberg series will lie above  $N' - 2$ . These can transfer two units of angular momentum. We have carried out such calculations up to  $N' - 4$ , and including various possible branches (*O, P, Q, R, S*). A basic assumption here is that all Rydberg states energetically capable of autoionization will do so.

The intensity of each transition is calculated by taking into account the Boltzmann rotational population, an electronic excitation probability varying as  $(n)^{-3}$ , and the Hönl-London factors. After computing a set of such energies and intensities corresponding to a given branch, and a given  $\Delta N$  (number of units of rotational angular momentum transferred), the transitions are sorted by energy and convoluted with a Gaussian function whose half width is equal to the instrumental resolution.

In Fig. 3, we compare four simulated spectra with the experimental one, plotted on a wave number energy scale. Each of the simulations is a *Q* branch in absorption<sup>8</sup>; they differ in the number of rotational quanta transferred, vary-

ing from  $N' - 1$  to  $N' - 4$ . A rather good correspondence between simulation and experiment occurs for  $\Delta N = -3$  or  $\Delta N = -4$ . Apart from some weak structure at  $\sim 93\,565$  and  $\sim 93\,585\text{ cm}^{-1}$  in the experimental spectrum, and the two rather intense features at  $\sim 94\,020$  and  $94\,110\text{ cm}^{-1}$  very close to the adiabatic ionization potential, both not present in the simulation, the other structural features match well. Thus, it appears as if one particular branch accounts for the bulk of the structure. The peaks are not spaced equally in energy. Only one juxtaposition of the simulation and the experimental curve provides a good match. With this choice, the simulated energy scale differs from the calibrated experimental energy scale by  $50\text{ cm}^{-1}$ . Hence, starting with an assumed ionization potential of  $11.66\text{ eV}$ , we derive an improved value of  $11.666 \pm 0.002\text{ eV}$ , which is essentially the value given by Huber and Herzberg.<sup>3</sup>

The two intense features straddle the ionization potential ( $11.666\text{ eV} \equiv 94\,090\text{ cm}^{-1}$ ). Such intense autoionizing features imply a low  $n^*$  state, converging to a higher ionization potential. Since they appear at about the same energy in DBr, they are more likely members of Rydberg series converging to the spin-orbit excited state ( $^2\Pi_{1/2}$ ), rather than to a vibrationally excited state. The close proximity of these states to the first ionization potential, where very high  $n^*$  states converging to  $X\ ^2\Pi_{3/2}$  are also expected, implies the possibility of strong mixing. This is the domain where MQDT calculations might rationalize these observations.

We have made a similar simulation for DBr. In Fig. 4, we compare this simulation (only the *Q* branch, with

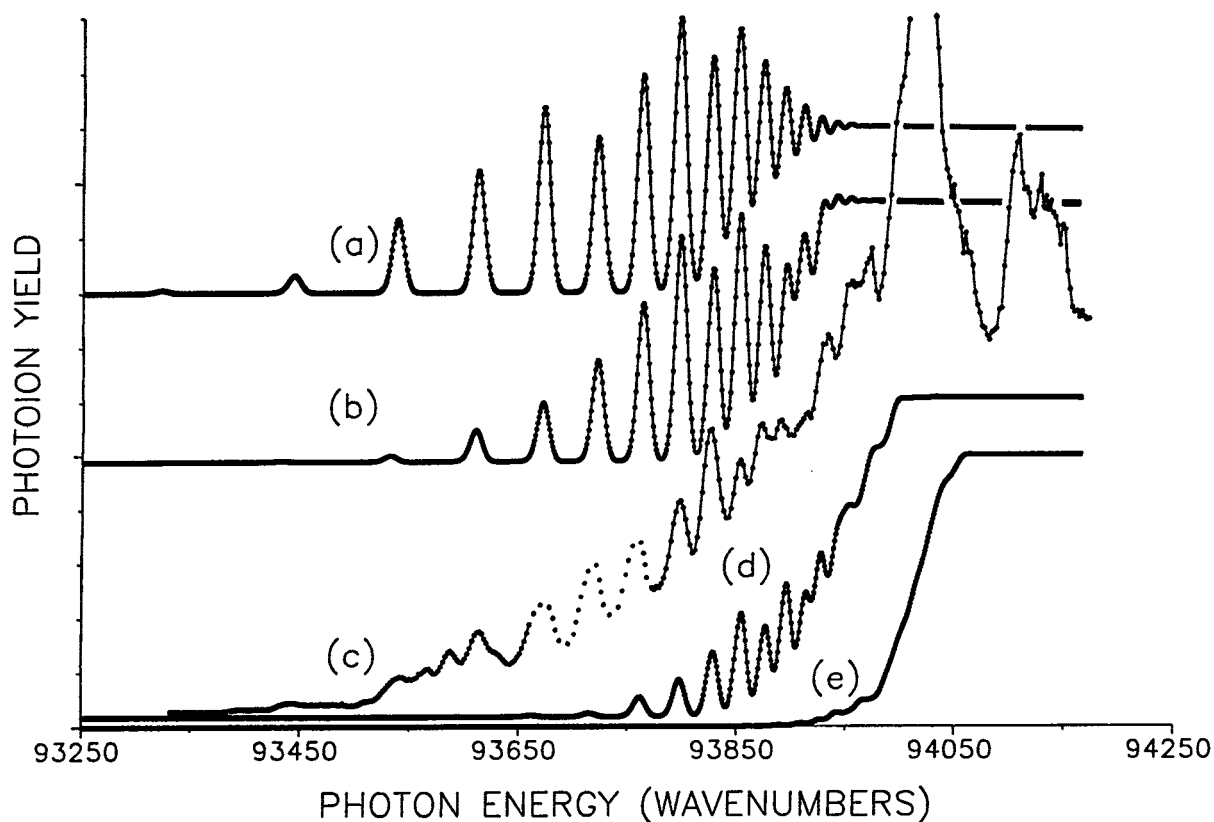


FIG. 3. Photoion yield curve of HBr below the adiabatic threshold compared with four simulations, all involving the  $Q$  branch (Ref. 8) in absorption. (a)  $\Delta N = -4$ ; (b)  $\Delta N = -3$ ; (c) Experimental spectrum: dotted portion ( $\sim 93\,670$ – $93\,720\text{ cm}^{-1}$ ) obtained with  $\text{H}_2$  light source, and is only approximate. (d)  $\Delta N = -2$ ; (e)  $\Delta N = -1$ .

$\Delta N = -4$  is shown) with the experimental data for DBr. A similar level of agreement is observed, and leads to IP (DBr) higher than IP (HBr) by  $21 \pm 6\text{ cm}^{-1}$ . This is about the difference expected ( $23\text{ cm}^{-1}$ ), when zero-point energies and lowest rotational terms are taken into account.

### B. Formal theory

Formally, the autoionization rate  $\Gamma$  from a state of quantum numbers  $n, l, N, J$  to the continuum of energy  $\epsilon'$  above the  $N'$  rotational level of the ion may be written

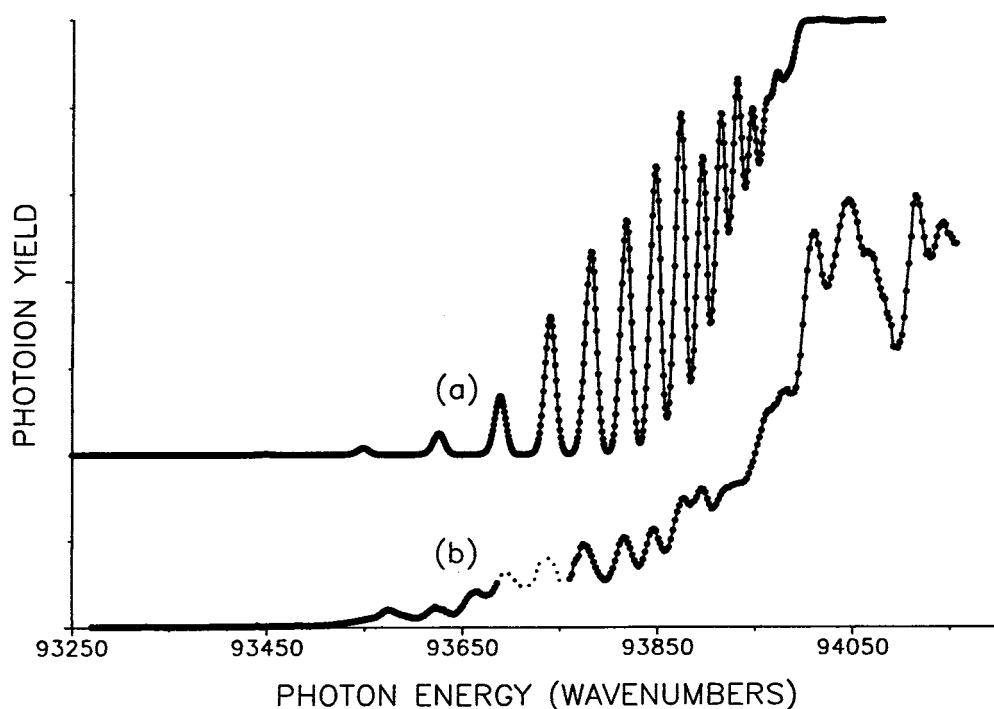


FIG. 4. Photoion yield curve of DBr below the adiabatic threshold compared with a simulation involving the  $Q$  branch (Ref. 8), with  $\Delta N = -4$  autoionization. (a)  $\Delta N = -4$  simulation; (b) Experimental spectrum: dotted portion ( $\sim 93\,670$ – $93\,700\text{ cm}^{-1}$ ) obtained with  $\text{H}_2$  light source, and is only approximate.

$$\Gamma = 2\pi |\langle nlNJ | V | \epsilon' l' N' J \rangle|^2. \quad (1)$$

The perturbation potential  $V$  is the interaction of the Rydberg electron with the core, i.e.,

$$V = \sum_{\text{core}} \frac{e_{\text{Ryd}} e_{\text{core}}}{|r - r_{\text{core}}|}. \quad (2)$$

Eyler and Pipkin<sup>9</sup> have developed this multipolar expansion for the case of  $\text{H}_2$ , where no odd multipoles appear. They have included the quadrupolar term, and a term involving the polarizability. In the present case of a heteronuclear system, we shall retain the dipolar and quadrupolar term, as done by Eyler,<sup>10</sup> but neglect all higher multipoles.

Thus,

$$V = V_d + V_q, \quad (3)$$

$$V_d = \frac{e_{\text{Ryd}}}{r_{\text{Ryd}}^2} \cdot C_0^{(1)}(e_{\text{Ryd}}) \cdot D, \quad (4)$$

$$D = \sum_{\text{core}} e_{\text{core}} r_{\text{core}} C_0^{(1)}(\text{core}), \quad (5)$$

$$V_q = \frac{e_{\text{Ryd}}}{r_{\text{Ryd}}^3} \cdot C_0^{(2)}(e_{\text{Ryd}}) \cdot Q, \quad (6)$$

$$Q = \sum_{\text{core}} e_{\text{core}} r_{\text{core}}^2 C_0^{(2)}(\text{core}), \quad (7)$$

where  $D$  is the electric dipole moment of the molecular ion core, and  $Q$  is the corresponding quadrupole moment. This expansion assumes the absence of core penetration for the Rydberg electron, which is dubious for  $l < 2$ .<sup>11</sup> The corresponding matrix elements are as follows:

$$H_d = -e \langle v' N' | D | v N \rangle \langle n' l' | r^{-2} | n l \rangle (-1)^{l' + N' + J} \begin{Bmatrix} J & N' & l' \\ 1 & l & N \end{Bmatrix} \delta_{J', J} \delta_{M', M},$$

$$\times (-1)^{l'} [(2l' + 1)(2l + 1)]^{1/2} \begin{bmatrix} l' & 1 & l \\ 0 & 0 & 0 \end{bmatrix} (-1)^{N'} [(2N' + 1)(2N + 1)]^{1/2} \begin{bmatrix} N' & 1 & N \\ 0 & 0 & 0 \end{bmatrix}, \quad (8)$$

with selection rules  $\Delta J = 0$ ,  $\Delta M_J = 0$ ,  $\Delta N = \pm 1$  and  $\Delta l = \pm 1$ .

$$H_q = -e \langle v' N' | Q | v N \rangle \langle n' l' | r^{-3} | n l \rangle (-1)^{l' + N' + J} \begin{Bmatrix} J & N' & l' \\ 2 & l & N \end{Bmatrix} \delta_{J', J} \delta_{M', M},$$

$$\times (-1)^{l'} [(2l' + 1)(2l + 1)]^{1/2} \begin{bmatrix} l' & 2 & l \\ 0 & 0 & 0 \end{bmatrix} (-1)^{N'} [(2N' + 1)(2N + 1)]^{1/2} \begin{bmatrix} N' & 2 & N \\ 0 & 0 & 0 \end{bmatrix}, \quad (9)$$

with selection rules  $\Delta J = 0$ ,  $\Delta M_J = 0$ ,  $\Delta N = 0, \pm 2$  and  $\Delta l = 0, \pm 2$ .

The matrix element  $H_d$  consists of a dipole moment of the molecular ion core, an electronic matrix element ( $1/r^2$ ) which can be taken to be hydrogenic, and an angular factor. To our knowledge, the dipole moment of  $\text{HBr}^+$  has not been measured, although that of  $\text{HBr}$  is 0.82 D.<sup>5</sup> Curtiss<sup>12</sup> has calculated  $\mu(\text{HBr}) = 1.13$  D, and  $\mu(\text{HBr}^+) = 1.59$  D. Assuming that the ratio of calculated and experimental dipole moments is approximately constant, we deduce  $\mu(\text{HBr}^+) = 1.15$  D, or 0.454 a. u. For the electronic matrix element, Mahon *et al.*<sup>13</sup> have approximated the related  $r^{-3}$  matrix element by

$$\langle nl | 1/r^3 | n'l \rangle = \frac{1}{n^{3/2}} \cdot \frac{1}{(n')^{3/2}} \cdot \frac{1}{(l + 1/2)^3} \quad (10)$$

and

$$\langle nl | 1/r^3 | n'l + 2 \rangle \cong \left[ \frac{1}{30} \right] \frac{1}{n^{3/2}} \cdot \frac{1}{(n')^{3/2}} \cdot \frac{1}{(l + 5/2)^3}. \quad (11)$$

A similar approximation yields

$$\langle nl | 1/r^2 | n'l \rangle = \frac{1}{n^{3/2}} \cdot \frac{1}{(n')^{3/2}} \cdot \frac{1}{(l + 1/2)} \quad (12)$$

and

$$\langle nl | 1/r^2 | n'l + 1 \rangle \cong \left[ \frac{1}{30} \right]^{1/2} \cdot \frac{1}{n^{3/2}} \cdot \frac{1}{(n')^{3/2}} \cdot \frac{1}{(l + 3/2)}. \quad (13)$$

These latter two expressions have been compared with direct calculations of the hydrogenic matrix elements for  $8p \rightarrow 8p$  and  $8p \rightarrow 10d$ , and were within 8.4% and 6.1%, respectively. Again following Mahon *et al.*,<sup>13</sup> the corresponding bound-free matrix elements for  $\epsilon \approx 0$ , for a continuum wave normalized per unit energy become

$$\langle nl | 1/r^2 | \epsilon l \rangle = \frac{1}{n^{3/2}} \cdot \frac{1}{(l + 1/2)} \quad (14)$$

and

$$\langle nl | 1/r^2 | \epsilon l + 1 \rangle \cong \left[ \frac{1}{30} \right]^{1/2} \cdot \frac{1}{n^{3/2}} \cdot \frac{1}{(l + 3/2)}. \quad (15)$$

We shall evaluate these matrix elements for the lowest  $l$  nonpenetrating state,<sup>11</sup>  $l = 3$ . In the dipole case, the angular factor is zero for  $l \rightarrow l$  transitions. For  $l \rightarrow l + 1$  and  $N \rightarrow N - 1$  transitions, the electronic matrix element for  $n = 16$  is 0.000 634, and the average of the angular factors is  $\sim 0.2$ . When combined with the dipole moment of  $\text{HBr}^+$ , one obtains  $\sim 5.76 \times 10^{-5}$  a. u. for the dipole matrix element,  $H_d$ .

The quadrupole moment of  $\text{HBr}^+$  has been calculated<sup>12</sup> to be  $Q_{zz} = -9.1$  a. u. From Eq. (9), the angular factors are

$\sim 0.1$  for  $l \rightarrow l$  transitions, and  $\sim 0.3$  for  $l \rightarrow l + 2$  transitions, both corresponding to  $N \rightarrow N - 2$  core transitions. The relevant electronic matrix elements [Eqs. (10) and (11)] for  $n = 16$  are  $\sim 3.64 \times 10^{-4}$  for  $l \rightarrow l$ , and  $\sim 3.13 \times 10^{-6}$  for  $l \rightarrow l + 2$ . Thus,  $l \rightarrow l$  matrix elements are favored over  $l \rightarrow l + 2$  matrix elements by a factor of  $\sim 100$ . For the favored case, the quadrupole matrix element  $H_q$  is  $\sim 3.3 \times 10^{-4}$  a.u., which is about a factor 6 larger than  $H_d$ . With this value of  $H_q$  Eq. (1) yields  $\Gamma \approx 6.91 \times 10^{-7}$  a.u., or (converting from a.u. to  $s^{-1}$ ),  $\sim 2.86 \times 10^{10}/s$ . The dipole matrix element then leads to  $\Gamma = 2.08 \times 10^{-8}$  a.u., or  $8.61 \times 10^8/s$ .

However, the dipole and quadrupole matrix element can only account for  $\Delta N = -1$  and  $\Delta N = -2$ ; the observed values are  $\Delta N \leq -3$ , although  $\Delta N = -1$  and  $\Delta N = -2$  may be occurring, but be masked in the region closer to threshold. To account for these larger transfers of angular momentum, we must either invoke higher moments or apply second-order perturbation theory. As Mahon *et al.*<sup>13</sup> have shown in their case, the latter appears more likely.

The matrix element in second-order perturbation theory may be written

$$\sum_j \frac{A_k \langle n_i N_i l_i | V_k | n_j N_j l_j \rangle}{E_i - E_j} A'_k \langle n_j N_j l_j | V'_k | \epsilon_f N_f l_f \rangle,$$

where  $V_k, V'_k$  can be either  $V_d$  or  $V_q$ ,  $A_k$  and  $A'_k$  represent the molecular terms (dipole or quadrupole),  $i$  and  $f$  refer to initial and final states, and the summation is over intermediate states  $j$ . One of these states will be more resonant than the others, and will dominate the summation. Let us consider a representative case—the aforementioned peak at (93 670  $\text{cm}^{-1}$ ). The largest contributor to this peak is calculated to be  $J'' = 8$ , (IP = 94 104.38  $\text{cm}^{-1}$ ) excited to  $n^* = 15.92$ , which requires  $h\nu = 93 671.40 \text{ cm}^{-1}$ . We take the initial step to be  $\Delta N = -2$  ( $V_k = V_q$ ), and examine the energy levels of the intermediate states. They will be Rydberg terms converging to an ionization potential two rotational quanta (253.08  $\text{cm}^{-1}$ ) lower, or 93 851.30  $\text{cm}^{-1}$ . The closest Rydberg level is 93 674.59  $\text{cm}^{-1}$ , corresponding to  $n^* = 24.92$ . The next closest is 93 659.51  $\text{cm}^{-1}$ , with  $n^* = 23.92$ . Thus, the summation in this case will be dominated by  $n_j = 24.92$ , with  $E_i - E_j = -3.19 \text{ cm}^{-1}$ . (We have examined several cases, corresponding to other peaks in the spectrum, and find  $E_i - E_j$  to range from  $\sim 0.3$  to  $\sim 3 \text{ cm}^{-1}$ , so the example chosen is not particularly favorable.) The first term in the numerator becomes

$$A_k \langle n_i N_i l_i | V_q | n_j N_j l_j \rangle = (9.1)(0.1) \frac{1}{(15.92)^{3/2}} \cdot \frac{1}{(24.92)^{3/2}} \cdot \frac{1}{(3.5)^3},$$

or  $2.69 \times 10^{-6}$ . With  $E_i - E_j = -3.19 \text{ cm}^{-1} = -14.5 \times 10^{-6}$  a.u., the ratio is  $-0.185$ . This fraction represents a part of the reduction in matrix elements when going from first to second-order perturbation theory.

The second term in the numerator can still be dipolar or quadrupolar. It will be reduced in magnitude from the previous (first-order) calculation, because  $n_j$  is higher. Thus, for the quadrupolar case

$$A'_k \langle n_j N_j l_j | V_q | \epsilon_f N_f l_f \rangle = (9.1)(0.1) \frac{1}{(24.92)^{3/2}} \cdot \frac{1}{(3.5)^3} = 1.71 \times 10^{-4}.$$

For the dipolar case,

$$A'_k \langle n_j N_j l_j | V_d | \epsilon_f N_f l_f \rangle \approx (0.454)(0.2) \left[ \frac{1}{30} \right]^{1/2} \times \left[ \frac{1}{24.92} \right]^{3/2} \cdot \left[ \frac{1}{4.5} \right] \approx 2.96 \times 10^{-5}.$$

Utilizing Eq. (1), we obtain

$$\Gamma_{QQ} = 6.25 \times 10^{-9} \text{ a.u.}, \text{ or } \sim 2.6 \times 10^8/s,$$

and

$$\Gamma_{QD} \approx 1.88 \times 10^{-10} \text{ a.u.}, \text{ or } \sim 7.8 \times 10^6/s,$$

where  $\Gamma_{QQ}$  refers to successive quadrupole steps, and  $\Gamma_{QD}$  corresponds to a quadrupole followed by a dipole transition. In the example given,  $\Gamma_{QD}$  is really 0, since 3 rotational quanta are insufficient for autoionization, but the relative magnitudes of  $\Gamma_{QQ}$  and  $\Gamma_{QD}$  are representative.

These rates may be considered conservative, since they depend sensitively on  $E_i - E_j$ , and more favorable cases exist. In any case, the calculation predicts that  $\Gamma_{QQ}$  will exceed  $\Gamma_{QD}$  by a factor of  $\sim 30$ . Since these rates can be considered competitive,  $\Gamma_{QQ}$  should dominate.

It may appear as if the direct quadrupole rate ( $\Delta N = -2$ ), which is about two orders of magnitude larger than the rate for  $\Delta N = -4$  obtained from second-order perturbation theory, will dominate. However, they will not compete in the same region of the spectrum. For example, in order that  $n \approx 16$  should lead to a simple quadrupole transition, the initial  $J''$  state must be 14. By contrast, the same  $n$ , but with  $J'' = 8$ , can lead to a  $\Delta N = -4$  transition. The ratio of Boltzmann and Hönl-London factors favors the  $J'' = 8$  transition by  $\sim 2$  orders of magnitude. Hence, the peak at  $\sim 93 670 \text{ cm}^{-1}$  is predominantly due to  $J'' = 8$ , with successively lesser contributions from higher  $J''$  states. The  $\Delta N = -2$  (and possibly also  $\Delta N = -1$ ) transitions will be localized in the near threshold regions.

In order that autoionization be detectable in our apparatus, it must occur within a few microseconds. As long as  $\Gamma$  exceeds  $\sim 10^6/s$ , the processes corresponding to  $\Delta N = -4$  (and to a lesser extent,  $\Delta N = -3$ ) should be observable.

## V. CONCLUSION

The ionization observed below the nominal ionization threshold in HBr and DBr cannot be explained as direct transitions to the continuum, since such transitions should not display peak structure. It can be explained as a manifestation of rotational autoionization. The possible influence of collisional autoionization has been explored over a substantial pressure range, without significant effect. One may contend that even at our lowest pressure, each excited state is collisionally ionized, implying exceedingly large cross sections. Even then, it would be necessary to explain the particular pattern observed.

There is good reason to believe that rotational autoion-

ization in the near threshold region may be a rather general phenomenon. Preliminary experiments with NO and HF tend to support this view. Prominent, structural ionization below threshold has been observed for HCl<sup>14</sup> and HI.<sup>15</sup> In the latter case, reported earlier from this laboratory, it was noted that "Rotational autoionization is probably significant in this region."

Although information regarding the dipole and quadrupole moments of molecular ions is sparse, the available data on the corresponding neutral species<sup>16</sup> suggest that the quadrupole term may usually have the larger magnitude (in a.u.).

The manner in which rotational autoionization manifests itself may be characteristically different for homonuclear and heteronuclear molecules, since the higher symmetry of the former imposes more restrictive selection rules. Spontaneous rotational autoionization in H<sub>2</sub> has been observed as window resonances. Theory<sup>17</sup> has shown that the photoabsorption transitions to these resonances correspond to  $\Delta J = +1$  (*R* transitions). The photoabsorption matrix element for these transitions is nearly zero, a consequence of the mixing of *npπ* and *npσ* dipole strengths in the transformation from Hund's case (b) to Hund's case (d), also called *l* uncoupling. Since the neutral and ionic states involved (<sup>1</sup>Σ<sub>g</sub><sup>+</sup> and <sup>2</sup>Σ<sub>g</sub><sup>+</sup>) are the same in H<sub>2</sub>, N<sub>2</sub> and the alkali dimers, as is the Rydberg electron (*l* = 1), the mechanism leading to *window* resonances should apply to all of these species, although it may be difficult to observe. In our recent study on N<sub>2</sub>,<sup>4</sup> we observed *peak* structure attributable to rotational autoionization, but it required a Stark field of ~10 V/cm. This has been interpreted<sup>4</sup> as field-induced autoionization corresponding to *Q* transitions ( $\Delta J = 0$ ). These *Q* transitions have relatively large dipole strengths, but the excited Rydberg states cannot autoionize spontaneously. However, the application of a weak electric field transforms the Rydberg electron into a mixture of *l* states, removing the restriction to autoionization. Preliminary experiments in this laboratory with F<sub>2</sub> and Cl<sub>2</sub> (which also have <sup>1</sup>Σ<sub>g</sub><sup>+</sup> neutral ground states and *p*-like Rydberg electrons, but a different ionic ground state) indicate that electric field effects are apparent here, as well.

Thus far, our experiments indicate that heteronuclear diatomic molecules display rotational autoionization in the absence of a field. We do not yet know if the magnitude of the electric dipole moment of the core is significant, or if it is sufficient to simply spoil the *D*<sub>∞h</sub> symmetry. It would be interesting to examine CO (isoelectronic with N<sub>2</sub>, but having a small dipole moment) or isotopic species such as <sup>14</sup>N<sup>15</sup>N and <sup>35</sup>Cl<sup>37</sup>Cl.

We have not yet examined polyatomic molecules for the possible occurrence of rotational autoionization. Here, the presence (in general) of three rotational constants may introduce complications to the analysis of the experimental data.

Lefebvre-Brion and Field<sup>18</sup> set a lower bound on the value of *n*\* required for rotational autoionization, i.e.,

$$n^* \geq \left[ \frac{R}{\Delta E} \right]^{1/2},$$

where *R* is the Rydberg constant, and  $\Delta E$  is the difference in energy between successive rotational states. Thus, for N<sub>2</sub>, with *B* ~ 2 cm<sup>-1</sup>,  $\Delta E_{0-2} \approx 6B \approx 12$  cm<sup>-1</sup>, they obtain *n*\* ≥ 96. However,  $\Delta E$  increase with *N*, thereby diminishing *n*\*. Hence, rotational autoionization should be most readily seen in high *N* states, with correspondingly lower *n*\* states. This deduction has some interesting consequences. In recent years, it has been tacitly assumed that cooling a sample (e.g., by supersonic expansion) would simplify the spectrum, and lead to a more unambiguous determination of the adiabatic ionization threshold. From the above analysis, it is clear that this makes the observation of rotational autoionization more difficult. A warmer sample, having a larger population of high *N* states inherently contains more information. If the resultant resolved autoionization peaks could be unambiguously assigned, one could infer an accurate adiabatic ionization potential. This procedure implies that the relevant rotational constants are well-known. Thus, in the present case we infer IP (HBr) = 11.666 ± 0.002 eV, assuming that the quantum defect remains constant, i.e.,  $\delta = 3.08$ .<sup>19</sup> A possible change in  $\delta$  by 0.5, which is about the maximum possible (modulo 1) can alter the result by ~0.001 eV.

Apart from the well-established case of H<sub>2</sub>, rotational autoionization has been inferred<sup>20</sup> as a possible mechanism (in addition to vibrational autoionization) for the creation of near-zero energy electrons in the Franck-Condon gap in some polyatomic molecules. However, the evidence for the latter is much less compelling than the analysis presented here, since only a single type of peak occurs, and it cannot easily be predicted when it will be seen. If the general analysis described in this paper is valid, rotational autoionization should be possible in other portions of the spectrum, but it may be masked by other processes. The near-threshold region may be the clearest one for its observation.

Finally, we note that one of the triad of peaks appearing just above threshold in the photoionization spectrum of HBr is predicted by an MQDT calculation<sup>1</sup> to be absent in DBr. We have examined both, and find that, although relative intensities change, the relevant peak persists in DBr.

## ACKNOWLEDGMENT

This research was supported by the U. S. Department of Energy, Office of Basic Energy Sciences, under Contract No. W-31-109-Eng-38.

<sup>1</sup>H. Lefebvre-Brion, P. M. Dehmer, and W. A. Chupka, *J. Chem. Phys.* **85**, 45 (1986).

<sup>2</sup>D. A. Shaw, D. Cvejanovic, G. C. King, and F. H. Read, *J. Phys.* **B 17**, 1173 (1984).

<sup>3</sup>K. P. Huber and G. Herzberg, *Molecular Spectra and Molecular Structure IV. Constants of Diatomic Molecules* (Van Nostrand Reinhold, New York, 1979). These authors considered photoelectron spectroscopic values of 11.71 ± 0.01 eV [D. C. Frost, C. A. McDowell, and D. A. Vroom, *J. Chem. Phys.* **46**, 4255 (1967)], 11.67 ± 0.01 eV [H. J. Lempka, T. R. Passmore, and W. C. Price, *Proc. London Ser. Soc. A* **304**, 53 (1968)], both using retarding field analyzer, and a photoionization value of 11.62 ± 0.01 eV [K. Watanabe, *J. Chem. Phys.* **26**, 542 (1957)]. They also mention the value 11.645 ± 0.005 eV obtained with a dispersive analyzer [J. Delwiche, P. Natalis, J. Momigny, and J. E. Collin, *J. Electron Spectrosc.* **1**, 219 (1972)].

- <sup>4</sup>J. Berkowitz and B. Ruscic, *J. Chem. Phys.* **93**, 1741 (1990) (previous paper).
- <sup>5</sup>R. D. Nelson, Jr., D. R. Lide, Jr., and A. A. Maryott, *Selected Values of Electric Dipole Moments for Molecules in the Gas Phase*, Natl. Stand. Ref. Data Serv., Natl. Bur. Stand. Circ. No. 10 (U.S. GPO, Washington, D.C., 1967).
- <sup>6</sup>S. T. Gibson, J. P. Greene, and J. Berkowitz, *J. Chem. Phys.* **83**, 4319 (1985).
- <sup>7</sup>B. Ruscic, J. P. Greene, and J. Berkowitz, *J. Phys. B* **17**, 1503 (1984).
- <sup>8</sup>To clarify our terminology for the  $Q$  branch, we assume that the  $\text{HBr}^+$ ,  $^2\Pi_{3/2}$  core acquires a Rydberg electron. Formally, the absorption transition can be considered  $\Delta\Lambda = +1$ . The  $Q$  branch, corresponding to  $\Delta J = 0$ , implies  $\Delta N = -1$ .
- <sup>9</sup>E. E. Eyler and F. M. Pipkin, *Phys. Rev. A* **27**, 2462 (1983).
- <sup>10</sup>E. E. Eyler, *Phys. Rev. A* **34**, 2881 (1986).
- <sup>11</sup>Mahon *et al.* (Ref. 12) have noted that autoionization rates for atoms calculated by expressions such as Eqs. (8) and (9), in which a separation has been made between the coordinates of the Rydberg electron and the core, are accurate as long as the Rydberg electron does not penetrate the ion core. "Furthermore, for the low  $l$  states for which penetration does occur, the autoionization rates are roughly equal to the lowest  $l$  nonpenetrating state" (Ref. 12).
- <sup>12</sup>L. A. Curtiss (private communication).
- <sup>13</sup>C. R. Mahon, G. R. Janik, and T. F. Gallagher, *Phys. Rev. A* **41**, 3746 (1990).
- <sup>14</sup>H. Lefebvre-Brion, P. M. Dehmer, and W. A. Chupka, *J. Chem. Phys.* **88**, 811 (1988).
- <sup>15</sup>J. H. D. Eland and J. Berkowitz, *J. Chem. Phys.* **67**, 5034 (1977).
- <sup>16</sup>A. A. Radzig and B. M. Smirnov, *Reference Data on Atoms, Molecules and Ion* (Springer, Berlin/Heidelberg, 1985), pp. 440-446.
- <sup>17</sup>G. Herzberg and Ch. Jungen, *J. Mol. Spectrosc.* **41**, 425 (1972).
- <sup>18</sup>H. Lefebvre-Brion and R. W. Field, *Perturbations in the Spectra of Diatomic Molecules* (Academic, New York, 1986), pp. 391-392.
- <sup>19</sup>If one tries to fit the five peaks in the region 93 800 to 93 895  $\text{cm}^{-1}$  into a Rydberg series, the best match is achieved with  $\delta = -0.8$  ( $n^* = 19.2, 20.2, \dots, 23.2$ ). This leads to an ionization potential lower by 10  $\text{cm}^{-1}$ , but gives a mismatch for the peaks at lower energy, regardless of the assumed rotational autoionization mechanism ( $\Delta N = -1, -2, -3, -4$ , or more). If one includes the peaks at lower energy, and allows  $\delta$  to be a variable, the best overall match is achieved for  $\delta \sim -0.1$ , and  $\Delta N = -4$  or more. Such a fit leads to the ionization potential reported here.
- <sup>20</sup>W. A. Chupka, P. J. Miller, and E. E. Eyler, *J. Chem. Phys.* **88**, 3032 (1988).